

# Global stability of empty and fluid-filled imperfect cylindrical shells

P.B. Gonçalves<sup>a,\*</sup>, Z.J.G.N. Prado<sup>b</sup>, F.M.A. Silva<sup>a</sup>

<sup>a</sup>Civil Engineering Department, Catholic University, PUC – Rio, 22453–900, Rio de Janeiro, RJ, Brazil

<sup>b</sup>Civil Engineering Department, UFG, 74605–200, Goiânia, GO, Brazil

## Abstract

Based on Donnell shallow shell equations, this work discusses the influence of geometric imperfections on the parametric instability and snap-through buckling of empty and fluid-filled cylindrical shells under axial loads. In particular, the influence of imperfections on the evolution of basins of attraction is studied in detail. As parameters are varied, basins of attraction undergo quantitative and qualitative changes that may affect seriously the safety and stability of the shell.

*Keywords:* Cylindrical shells; Fluid–structure interaction; Parametric instability; Geometric imperfections; Global instability; Dynamic buckling

## 1. Introduction

A detailed review of studies on geometrically nonlinear vibrations and dynamic instability of empty and fluid-filled cylindrical shells is found in Amabili and Païdoussis [1]. Recently, Gonçalves and Del Prado [2] and Pellicano and Amabili [3] studied the dynamic instability of simply supported circular cylindrical shells subjected to harmonic axial loads. In the present study, a low-dimensional model that retains the essential nonlinear terms is used to study the effect of initial imperfections on the nonlinear oscillations and instabilities of the shell. To study the nonlinear behavior of the shell, several numerical strategies are used to obtain time response, Poincaré maps, bifurcation diagrams, and basins of attraction. The fluid is modeled as nonviscous and incompressible.

## 2. Problem formulation

Consider a thin-walled fluid-filled circular cylindrical shell of radius  $R$ , length  $L$ , and thickness  $h$  made of an elastic, homogeneous, and isotropic material with Young's modulus  $E$ , Poisson ratio  $\nu$ , and mass per unit area  $M$ . The axial, circumferential, and radial coordinates are denoted by, respectively,  $x$ ,  $y$ , and  $z$ , and the

corresponding displacements on the shell surface are, in turn, denoted by  $u$ ,  $v$ , and  $w$ . The nonlinear equations of motion based on Donnell shallow shell theory, in terms of a stress function  $f$  and the transversal displacement  $w$ , are given by [2]:

$$M \ddot{w} + \beta_1 \dot{w} + \beta_2 \nabla^4 \dot{w} + D \nabla^4 w = p_h R + F_{,yy} w_{,xx} + F_{,xx} \left( w_{,yy} \frac{1}{R} \right) - 2F_{,xy} w_{,xy} \quad (1)$$

$$\frac{1}{Eh} \nabla^4 f = \left[ -\frac{1}{R} w_{d,xx} + (-w_{i,xx} w_{d,yy} - w_{d,xx} w_{i,yy} - w_{d,xx} w_{d,yy}) + 2w_{i,xy} w_{d,xy} + w_{d,xy}^2 \right] \quad (2)$$

where  $F = f^F + f$ ,  $f^F = -\frac{1}{2} P_0 y^2 - \frac{1}{2} P_1 \cos(\omega t) y^2$ ,  $P(t) = P_0 + P_1 \cos(\omega t)$ ,  $w_i$  are the initial geometric imperfections,  $p_h$  is the fluid pressure,  $\nabla^4$  is the biharmonic operator,  $\beta_1$  and  $\beta_2$  are damping coefficients, and  $D$  is the flexural rigidity defined as  $D = Eh^3/12(1-\nu^2)$ . Also,  $P_0$  is the uniform static load applied along the edges  $x=0, L$ ,  $P_1$  is the magnitude of the harmonic load,  $t$  is time, and  $\omega$  is the forcing frequency.

The lateral deflection  $w$  can be described generally as [2,4]:

$$W = \sum_{i=1,3,5} \sum_{j=1,3,5} W_{ij} \cos(in\theta) \sin(jm\pi\zeta) + \sum_{k=0,2,4} \sum_{l=0,2,4} W_{ij} \cos(kn\theta) \cos(lm\pi\zeta) \quad (3)$$

\* Corresponding author. Tel.: +55 21 3114 1188; Fax: +55 21 3114 1195; E-mail: paulo@civ.puc-rio.br

where  $n$  is the number of waves in the circumferential direction of the basic buckling or vibration mode, and  $m$  is the number of half-waves in the axial direction,  $\theta = y/R$  and  $\varsigma = x/L$ .

The initial geometric imperfections are considered as:

$$W_i = \Xi_{11} \cos(n\theta) \sin(m\pi\varsigma) + \Xi_{02} \cos(2m\pi\varsigma) \quad (4)$$

where  $\Xi_{11}$  and  $\Xi_{02}$  are the amplitudes of the geometric imperfections.

The irrotational motion of an incompressible and nonviscous fluid can be described by a velocity potential  $\phi(x,r,\theta, t)$ , which must satisfy the Laplace equation. The hydrodynamic fluid pressure is [4]:

$$p_h = \zeta_{11,\tau\tau} m_a \cos(n\theta) \sin(m\pi\varsigma), \text{ with } m_a = (\rho_F R) \left\{ m\pi\varsigma \left[ \frac{I_{n-1}(m\pi\varsigma)}{I_n(m\pi\varsigma)} - \frac{n}{m\pi\varsigma} \right] \right\}^{-1} \quad (5)$$

where  $m_a$  is the added mass due to the fluid contained in shell,  $\rho_F$  is the density of the fluid,  $\rho_S$  is the shell material density, and  $I_{n-1}$  and  $I_n$  are Bessel functions.

### 3. Numerical results

Consider a thin cylindrical shell with  $h=0.002$  m,  $R=0.2$  m,  $L=0.4$  m,  $E=2.1 \times 10^8$  kN/m<sup>2</sup>,  $\nu=0.3$ ,  $M=78.5$  kg/m<sup>2</sup>, and  $\beta_1=2\varepsilon M\omega_o$ , with  $\varepsilon=0.003$  (fluid-filled shell) and  $\varepsilon=0.0008$  (empty shell), and  $\beta_2=\eta D$  with  $\eta=0.0001$ ,  $\rho_s=7850$  kg/m<sup>3</sup>, and  $\rho_f=2450$  kg/m<sup>3</sup>. For this geometry, the lowest natural frequency occurs for  $(n,m)=(5,1)$ . Fig. 1 shows the evolution of the basin of attraction of the perfect shell for increasing values of the forcing amplitude  $\Gamma_1$  ( $\Gamma_1 = P_1/P_{cr}$ ). The associated bifurcation diagram is shown in Fig. 1a. The black area corresponds to the fundamental trivial solution, the light and dark gray areas correspond to the

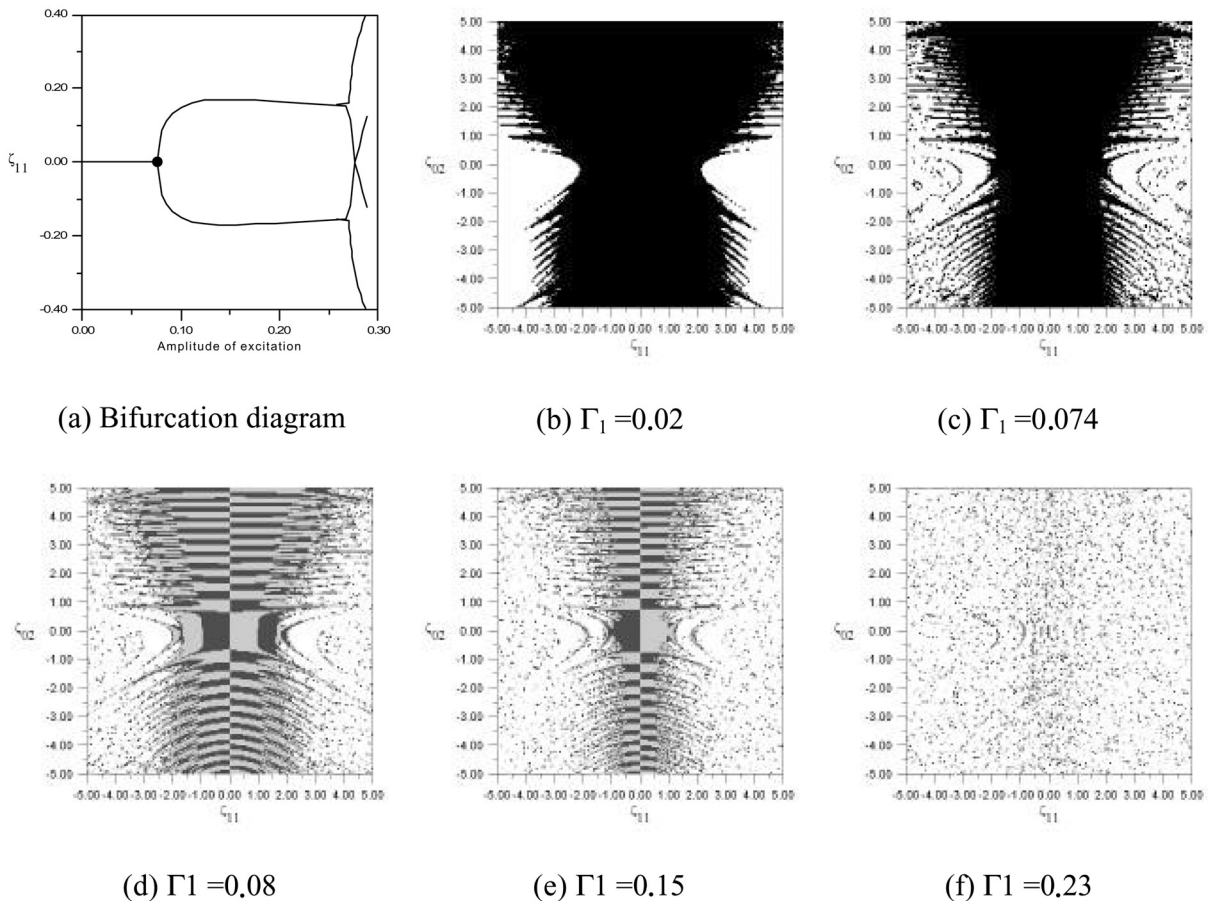


Fig. 1. Cross-sections of the basins of attraction for increasing values of the forcing amplitude  $\Gamma_1$  of the fluid-filled cylindrical shell.  $\Gamma_0 = 0.80$  and  $\Omega = 0.65$ . (a) Bifurcation diagram. (b)  $\Gamma_1 = 0.02$ . (c)  $\Gamma_1 = 0.074$ . (d)  $\Gamma_1 = 0.08$ . (e)  $\Gamma_1 = 0.15$ . (f)  $\Gamma_1 = 0.23$ .

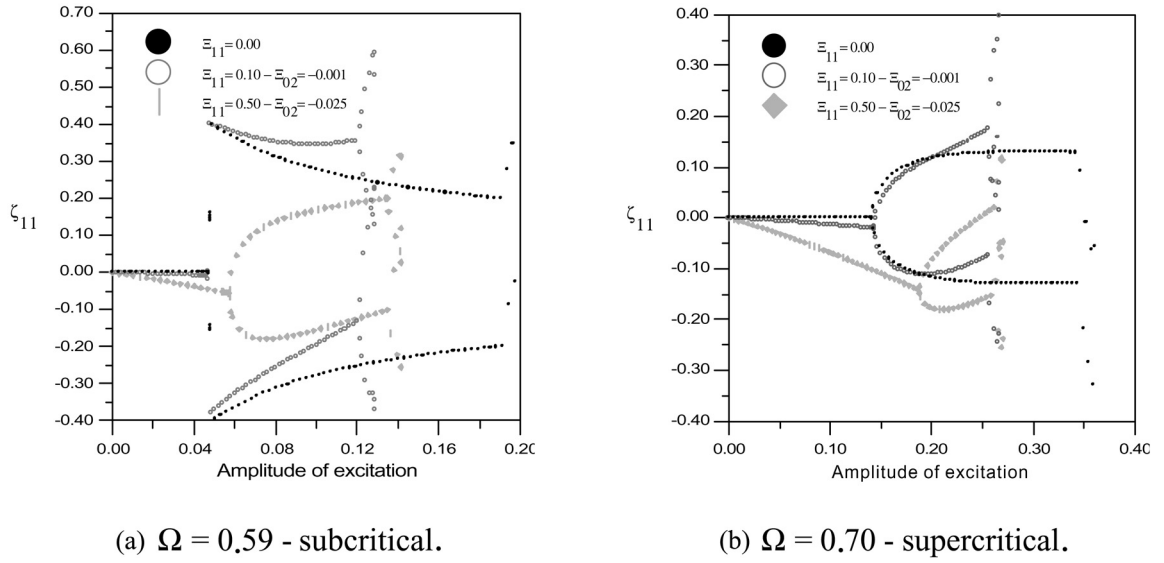


Fig. 2. Influence of geometric imperfections on the bifurcation diagrams – principal parametric instability region. Geometric imperfection in modes  $\Xi_{11}$  and  $\Xi_{02}$ .  $\Gamma_0 = 0.80$ . (a)  $\Omega = 0.59$  – subcritical. (b)  $\Gamma = 0.70$  – supercritical.

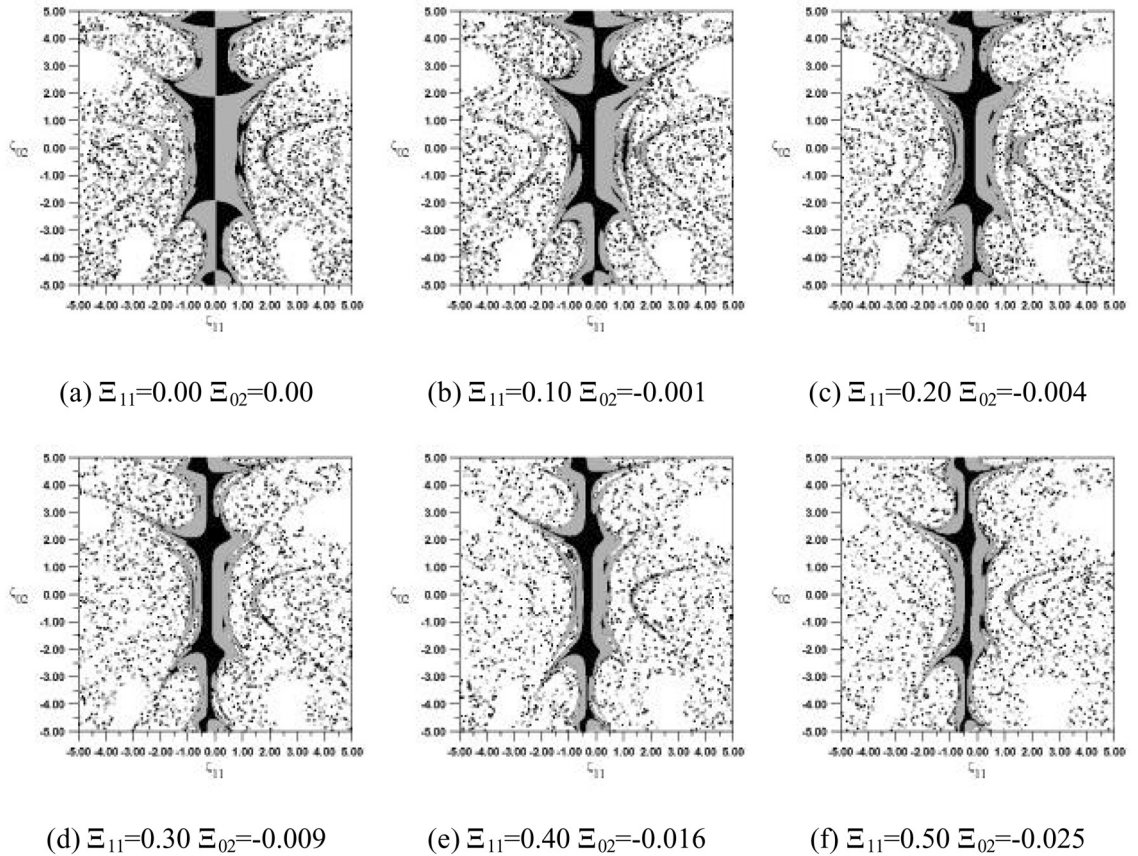


Fig. 3. Basins of attraction for increasing values of geometric imperfections.  $\Omega = 0.70$ ,  $\Gamma_0 = 0.80$  e  $\Gamma_1 = 0.20$ .  $\Xi_{11}^2/10$  (a)  $\Xi_{11} = 0.00$   $\Xi_{02} = 0.00$ . (b)  $\Xi_{11} = 0.10$   $\Xi_{02} = -0.001$ . (c)  $\Xi_{11} = 0.20$   $\Xi_{02} = -0.004$ . (d)  $\Xi_{11} = 0.30$   $\Xi_{02} = -0.009$ . (e)  $\Xi_{11} = 0.40$   $\Xi_{02} = -0.016$ . (f)  $\Xi_{11} = 0.50$   $\Xi_{02} = -0.025$ .

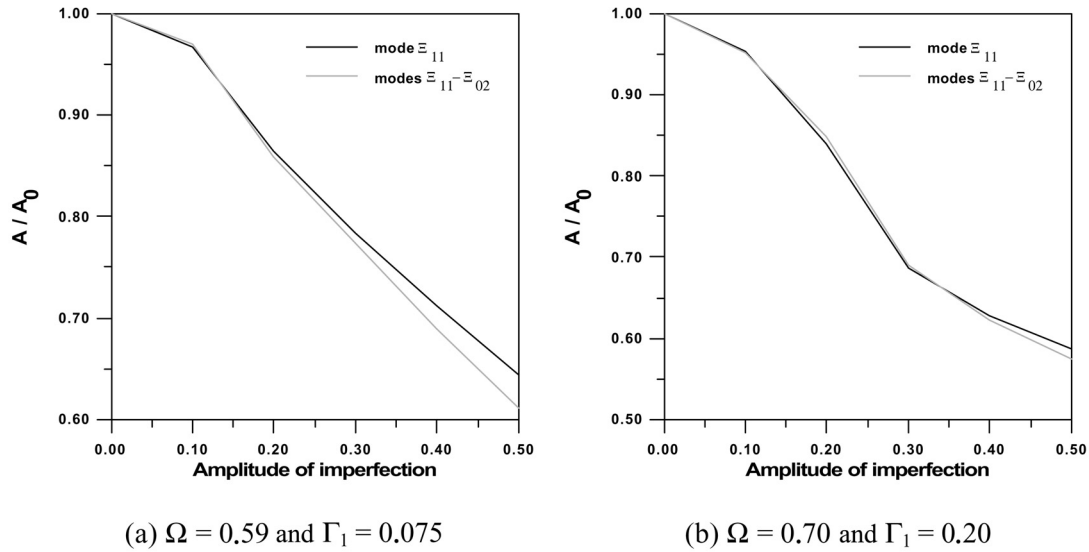


Fig. 4. Erosion of the stable region of the basin of attraction as a function of the imperfection amplitude. (a)  $\Omega = 0.59$  and  $\Gamma_1 = 0.075$ . (b)  $\Omega = 0.70$  and  $\Gamma_1 = 0.20$ .

period-two stable solutions within the prebuckling well, while the white area corresponds to escape (snap-through buckling). As  $\Gamma_1$  increases, the region associated with the stable solutions decreases and a rapid erosion is observed. Also, after a certain critical value, the whole basin of attraction becomes fractal. So, the response becomes very sensitive to the initial conditions and the steady-state response is unpredictable. Fig. 2 illustrates the influence of imperfections on two typical bifurcation diagrams of the principal region of parametric instability. Fig. 3 shows the evolution of the basin of attraction for increasing values of geometric imperfections and  $\Omega = 0.70$ ,  $\Gamma_0 = 0.80$ , and  $\Gamma_1 = 0.20$ . In these cross-sections of the four-dimensional phase space ( $\xi_{11} = \xi_{02} = 0.0$ ), the black and gray regions correspond to perturbations that produce stable period-two responses and the white region corresponds to initial conditions that lead to escape from the prebuckling potential well. The geometric imperfections have a high influence on the topology of the basin of attraction. When the imperfections increase, the basin that initially is symmetric in  $\xi_{11}$  begins to show a strong asymmetry in  $\xi_{11}$ . Again, the stable basin of attraction is eroded swiftly as the imperfection magnitude increases. Fig. 4 shows the variation of the stable area of the basin of attraction as a function of the imperfection magnitude.

#### 4. Concluding remarks

Based on Donnell's shallow shell equations, an accurate low-dimensional model is derived and applied to the study of the nonlinear vibrations of an axially loaded empty and fluid-filled imperfect circular cylindrical shell. The evolution and erosion of transient and permanent basin boundaries are analyzed, and their influence on the safety of the shell is discussed. Usually basin boundaries become fractal. This, together with the presence of catastrophic subcritical bifurcations, makes the shell very sensitive to initial conditions, uncertainties in system parameters, and initial imperfections.

#### References

- [1] Amabili M, Païdoussis MP. Review of studies on geometrically nonlinear vibrations and dynamics of circular cylindrical shells and panels, with and without fluid-structure interaction. *Appl Mech Rev ASME* 2003;56:349–381.
- [2] Gonçalves PB, Del Prado JGN. Nonlinear oscillations and stability of parametrically excited cylindrical shells. *Mechanica* 2002;37:569–597.
- [3] Pellicano F, Amabili M. Stability and vibration of empty and fluid-filled circular cylindrical shells under static and periodic axial loads. *Int J Solids Struct* 2003;40:3229–3251.
- [4] Gonçalves PB, Batista RC. Non-linear vibration analysis of fluid-filled cylindrical shells. *J Sound Vibrat* 1988;127:133–143.